J|A|C|S ARTICLES

Published on Web 07/13/2009

Octanuclear Copper(I) Clusters Inscribed in a Se_{12} Icosahedron: Anion-Induced Modulation of the Core Size and Symmetry

C. W. Liu,*,† Bijay Sarkar,† Yao-Jheng Huang,† Ping-Kuei Liao,† Ju-Chun Wang,‡ Jean-Yves Saillard,*,§ and Samia Kahlal§

Department of Chemistry, National Dong Hwa University, Hualien, Taiwan 97401, R.O.C., Department of Chemistry, Soochow University, Taipei, Taiwan 111, R.O.C., and UMR-CNRS 6226 "Sciences Chimiques de Rennes", Université de Rennes 1, 35042 Rennes cedex, France

Received May 20, 2009; E-mail: chenwei@mail.ndhu.edu.tw; saillard@univ-rennes1.fr

Abstract: Synthesis and structural characterization of an octanuclear Cu(I) cluster $[Cu_8\{Se_2P(O^iPr)_2\}_6](PF_6)_2$ (**1**) with an empty Cu_8 cubic core involving diisopropyl diselenophosphate (dsep) ligand has been demonstrated despite its high tendency to abstract anions even from the traces of impurities in the solvent. Reaction of **1** with anion sources (Bu_4NF for F^-; $NaBH_4$ for H^-, and NaSH for S^{2-}) in a 1:1 ratio produced anion-centered Cu_8 clusters with a formula $[Cu_8(X)\{Se_2P(O^iPr)_2\}_6](PF_6)$ (X = F, **2a**; H, **3a**; D, **3a′**) and $[Cu_8(S)\{Se_2P(O^iPr)_2\}_6]$ (**4**) in high yields. In addition, fluoride- and hydride-centered Cu_8^I clusters $[Cu_8(X)\{Se_2P(OEt)_2\}_6](PF_6)$ (X = F, **2b**; H, **3b**) could be generated in ~80% yield by direct reaction of $[Cu(CH_3CN)_4](PF_6)$, $NH_4Se_2P(OEt)_2$, and the anion sources (Bu_4NF for F^-; $NaBH_4$ for H^-) in 8:6:1 ratio. Whereas the structural elucidation of complexes **2** and **4** revealed an anion-centered cubic Cu_8 core surrounded by six dsep ligands, it was a tetracapped tetrahedral copper framework with a hydride in the center in compounds **3**. All Cu···Cu distances along either the edge of the cube in **2** and **4** or the tetracapped tetrahedron in **3** are shorter than those identified in **1**. Although the cubic (or spherical) contraction of the copper framework that was identified in a series of closed-shell anion-centered (except a hydride) Cu_8 cube having T_h symmetry could be explained by the existence of strong anion−cation attractions, it was definitely a surprise that the hydride, which is the smallest closed-shell anion and spherical too, induced a tetrahedral contraction of four out of the eight Cu atoms in the empty cube **1**, resulting in a tetracapped-tetrahedral geometry and reducing the symmetry to T from T_h. Furthermore the fact that the encapsulated anion induced modulation of the copper core size and symmetry was fully reproduced by DFT calculations on model compounds. To the best of our knowledge, this demonstrated the first example of the reduction of molecular symmetry (from T_h to T) simply by changing the encapsulated species without altering the general bonding pattern of the surrounding ligands. We also demonstrated that the hydride can easily replace other anions (Cl^-, Br^-, F^-, S^{2-}, Se^{2-}) in a very facile manner to produce hydride-centered species. Eventually, compounds **3** were stable in the presence of other anions, and hydride/deuteride exchange could not be achieved.

Introduction

Anion recognition[1−4] by molecular/supramolecular receptors has attracted much attention in the past decade with increasing demand for selective anion receptors and sensors that can allow the detection of particular species because of the high importance of anions in biological systems[5−10] as well as the harmful effects of anions on the environment, viz., anionic pollutants.[11−14] Surprisingly, most of the receptors are either entirely organic in nature or an organic part of the metal complexes having recognition capability. Though metal ions have a formal positive charge on them in complexes, entrapment of an anion solely by metal ions is limited. In this respect, octanuclear Cu(I)

† National Dong Hwa University.
‡ Soochow University.
§ Université de Rennes 1.

(1) Brown, A.; Mullen, K. M.; Ryu, J.; Chmielewski, M. J.; Santos, S. M.; Felix, V.; Thompson, A. L.; Warren, J. E.; Pascu, S. I.; Beer, P. D. *J. Am. Chem. Soc.* **2009**, *131*, 4937–4952.
(2) Steed, J. W. *Chem. Soc. Rev.* **2009**, *38*, 506–519.
(3) Beer, P. D.; Gale, P. A. *Angew. Chem., Int. Ed.* **2001**, *40*, 486–516.
(4) Edited by Gale, P. A. *Coord. Chem. Rev.* **2006**, *250*, 2917–3244.
(5) Burkhard, P.; Tai, C.-H.; Jansonius, J. N.; Cook, P. F. *J. Mol. Biol.* **2000**, *303*, 279–286.
(6) Tai, C.-H.; Burkhard, P.; Gani, D.; Jenn, T.; Johnson, C.; Cook, P. F. *Biochemistry* **2001**, *40*, 7446–7452.
(7) Ashcroft, F. M. *Ion Channels and Disease*; Academic Press: San Diego, London, 2000.
(8) Burlington, B. T.; Widlanski, T. S. *J. Org. Chem.* **2001**, *66*, 7561–7567.
(9) Berg, J. M. *Acc. Chem. Res.* **1995**, *28*, 14–19.
(10) Puglisi, J. D.; Chen, L.; Frankel, A. D.; Williamson, J. R. *Proc. Natl. Acad. Sci. U.S.A.* **1993**, *90*, 3680–3684.
(11) Oliver, S. R. J. *Chem. Soc. Rev.* **2009**, *38*, 1868–1881.
(12) Delée, W.; O'Neill, C.; Hawkes, F. R.; Pinheiro, H. M. *J. Chem. Technol. Biotechnol.* **1998**, *73*, 323–335.
(13) Beigel, C.; Barriuso, E.; Calvet, R. *Pestic. Sci.* **1998**, *54*, 52–60.
(14) Bringas, E.; Román, M. F. S.; Ortiz, I. *J. Chem. Technol. Biotechnol.* **2006**, *81*, 1829–1835.

 10.1021/ja904089t CCC: $40.75

clusters involving phosphorus-chalcogenide are able to encapsulate a variety of anions such as Cl^-, Br^-, Se^{2-}, S^{2-}, etc.[15−21]

Incorporation of an elementary ion into the center of a centrosymmetric metal cluster or cage with cubic geometry usually retains the original symmetry of the cluster. Examples can be identified from several well-elucidated structures such as Zr_6AX_{12} (A = H, Be, B, C, Mn, etc.) and $[Co_9(Te)_6(CO)_8]$ in O_h symmetry,[22−24] $[Cu_8(X)\{E_2PR_2\}_6]^{n+}$ [X = Cl, Br ($n = 1$) and S, Se ($n = 0$); E = S, Se][15−21] in T_h symmetry, and $M@Pb_{12}^{2-}$ (M = Ni, Pd, Pt) in I_h symmetry.[25] Surprisingly none of these molecules mentioned above has been prepared directly from its empty metal framework. However, the size of metallic core may be varied with changes in both radius and charge of the encapsulating atom/ion. For example, the average edge length of the copper cube in $[Cu_8(Cl)\{Se_2P(O^iPr)_2\}_6]^+$ is ∼0.04 Å shorter than those in $[Cu_8(Br)\{Se_2P(O^iPr)_2\}_6]^+$ as the atomic radius of Br^- is greater than Cl^-.[15,16] On the other hand, for Se^{2-} and Br^- anions, which have comparable covalent radii (∼1.20 Å),[26] the difference in charge forced the selenide-centered copper cube to adopt a smaller size with the Cu···Cu distances in $[Cu_8(Se)\{Se_2P(O^iPr)_2\}_6]$ ranging from 2.859 to 2.974 Å,[17] whereas the Cu···Cu distances in $[Cu_8(Br)\{Se_2P(O^iPr)_2\}_6]^+$ are in the range of 3.139−3.225 Å.[16] Nevertheless, in all of these aforementioned clusters the geometry of the cubic framework does not alter a lot upon shrinkage of the cage when different guests are accommodated. Thus this type of shrinkage is associated with a spherical (or cubic) contraction.

Herein we demonstrate for the first time that anion-centered Cu_8 cubic clusters in T_h symmetry can be obtained directly by the reaction of closed-shell anions and a precursor with an empty metallic cage, $[Cu_8\{Se_2P(O^iPr)_2\}_6]^{2+}$, **1**. We further demonstrated that the anion recognition can be extended to the hydride and, upon addition of the smallest closed-shell anion, a hydride, which is spherical too, can also cause shrinkage of the copper cage but not in a spherical manner. Thus the cubic copper core in **1** with T_h symmetry undergoes a tetrahedral contraction resulting in a tetracapped-tetrahedral core in $[Cu_4(\mu_4\text{-}H)(\mu_3\text{-}Cu)_4\{Se_2P(O^iPr)_2\}_6]^+$, **3a**. In this process the center of symmetry was removed from the centro-symmetric cluster **1**. The irreversible conversion of a cluster with T_h symmetry to another with T symmetry simply by introducing the guest anion indeed provides a remarkable example of symmetry breaking and to the best of our knowledge there is no precedent for such a phenomenon. Furthermore the syntheses and characterizations of fluoride- and sulfide-centered clusters, $[Cu_8(\mu_8\text{-}F)\{Se_2P(O^iPr)_2\}_6]^+$, **2a** and $[Cu_8(\mu_8\text{-}S)\{Se_2P(O^iPr)_2\}_6]$, **4** obtained from **1** have been described herein. Ethyl homologues of both fluoride- and hydride-centered species $[Cu_8(\mu_8\text{-}F)\{Se_2P(OEt)_2\}_6]^+$, **2b** and $[Cu_4(\mu_4\text{-}H)(\mu_3\text{-}Cu)_4\{Se_2P(OEt)_2\}_6]^+$, **3b** were prepared directly from the reaction of the individual components and elucidated structurally by X-ray diffraction. DFT calculations performed on a series of model compounds fully confirmed the experimental results, i.e., the shrinkage of the copper cage with respect to the size of the encapsulated anion and the particular case of the cage tetrahedral contraction when the anion is a hydride.

Results and Discussion

An octanuclear cubic copper cluster, $[Cu_8\{Se_2P(O^iPr)_2\}_6](PF_6)_2$, **1**, is formed by the reaction of 4 equiv of $[Cu(CH_3CN)_4]PF_6$ and 3 equiv of $NH_4Se_2P(OR)_2$ in acetone, whereas their equimolar reaction produced $[Cu_4\{Se_2P(O^iPr)_2\}_4]$, which was reported previously.[27] Upon further reaction of **1** with 1 equiv of Bu_4NF in acetone, the F^- ion could be entrapped by the cubic copper cluster to form monocationic $[Cu_8(F)\{Se_2P(O^iPr)_2\}_6]^+$, **2a**, the solid-state structure of which has never been reported. In addition, both chloride- and bromide-centered cubic copper clusters,[15,16] which have been reported by this group and synthesized via the reaction of copper salts, diselenophosphate (dsep) ligands, and a source of halides (Bu_4NX, X = Cl, Br) in a 4:3:1 ratio, can also be obtained in high yield by the reaction $[Cu_8\{Se_2P(O^iPr)_2\}_6](PF_6)_2$, **1** and the halide sources following a similar reaction as fluoride. On the other hand, the ethyl homologue $[Cu_8(F)\{Se_2P(OEt)_2\}_6](PF_6)$, **2b** could be further isolated from a direct reaction of $[Cu(CH_3CN)_4]PF_6$, $NH_4[Se_2P(OEt)_2]$ and Bu_4NF in a 8:6:1 ratio and was also crystallographically characterized. At this point, we were curious about the probable synthesis and geometry of an octametallic copper cluster upon the encapsulation of a hydride, the smallest closed-shell anion. Thus stirring of 1 equiv of $NaBH_4$ (and $NaBD_4$) with compound **1** in THF for 10 min produced a brown-yellow residue with a molecular formula of $[Cu_8(H)\{Se_2P(O^iPr)_2\}_6](PF_6)$, **3a** and $[Cu_8(D)\{Se_2P(O^iPr)_2\}_6](PF_6)$, **3a′**, respectively. On the other hand, reaction of the ethyl homologue of dsep ligand $NH_4[Se_2P(OEt)_2]$ with copper salt and $NaBH_4$ in THF produces $[Cu_8(H)\{Se_2P(OEt)_2\}_6](PF_6)$, **3b**, which showed a structure very similar to that of **3a** (see next section). Reaction of **1** with NaSH in acetone again produced $[Cu_8(S)\{Se_2P(O^iPr)_2\}_6]$, **4**, the neutral octanuclear copper cluster with the S^{2-} entrapped inside the copper cage. It is noted that Na_2S could not be utilized for the entrapment of sulfide by **1**, partly because its higher pH may not be suitable for the reaction in the system. Previously Rauchfuss et al. used NaSH as the source of sulfide to obtain $[(cymene)_4Ru_5S_4](PF_6)_2$ via the formation of $[(cymene)_6Ru_9S_8](PF_6)_2$ and subsequent reaction with $[(cymene)_2Ru_3S_2(NCMe)_3]^{2+}$ in situ.[28]

All clusters reported in this article have been obtained in high yield (**1**−**3**, ∼80%; **4**, 67%).

Crystallography. Compound 1. Single crystal X-ray diffraction revealed the cubic copper framework in **1** (Figure 1) in which each square face of the copper cube is capped by a dsep ligand in a tetrametallic-tetraconnective (μ_2, μ_2) coordination

(15) Liu, C. W.; Hung, C.-M.; Santra, B. K.; Chen, H.-C.; Hsueh, H.-H.; Wang, J.-C. *Inorg. Chem.* **2003**, *42*, 3216–3220.
(16) Liu, C. W.; Hung, C.-M.; Santra, B. K.; Chu, Y. H.; Wang, J.-C.; Lin, Z. *Inorg. Chem.* **2004**, *43*, 4306–4314.
(17) Liu, C. W.; Chen, H.-C.; Wang, J.-C.; Keng, T.-C. *Chem. Commun.* **1998**, 1831–1832.
(18) Liu, C. W.; Irwin, M. D.; Mohamed, A. A.; Fackler, J. P., Jr. *Inorg. Chim. Acta* **2004**, *357*, 3950–3956.
(19) Liu, C. W.; Hung, C.-M.; Chen, H.-C.; Wang, J.-C.; Keng, T.-C.; Guo, K. *Chem. Commun.* **2000**, 1897–1898.
(20) Lobana, T. S.; Wang, J.-C.; Liu, C. W. *Coord. Chem. Rev.* **2007**, *251*, 91–110.
(21) Fackler, J. P., Jr. *Inorg. Chem.* **2002**, *41*, 6959–6972.
(22) Simon. A. In *Clusters and Colloids: From Theory to Applications*; Schmid, G., Ed.; VCH: New York, 1994; Chapter *5*, p 373.
(23) Welch, E. J.; Long, J. R. *Prog. Inorg. Chem.* **2005**, *54*, 1.
(24) Bencharif, M; Cador, O.; Cattey, H.; Ebner, A.; Halet, J.-F.; Kahlal, S.; Meier, W.; Mugnier, Y.; Saillard, J.-Y.; Schwarz, P.; Trodi, F. Z.; Wachter, J.; Zabel, M. *Eur. J. Inorg. Chem.* **2008**, 1959–1968.
(25) Esenturk, E. N.; Fettinger, J.; Eichhorn, B. *J. Am. Chem. Soc.* **2006**, *128*, 9178–9186.
(26) Cordero, B.; Gómez, V.; Platero-Prats, A. E.; Revés, M.; Echeverría, J.; Cremades, E.; Barragán, F.; Alvarez, S. *Dalton Trans.* **2008**, 2832–2838.
(27) Hsu, Y.-J.; Hung, C.-M.; Lin, Y.-F.; Liaw, B.-J.; Lobana, T. S.; Lu, S.-Y.; Liu, C. W. *Chem. Mater.* **2006**, *18*, 3323–3329.
(28) Kuhlman, M. L.; Rauchfuss, T. B. *Organometallics* **2004**, *23*, 5085–5087.

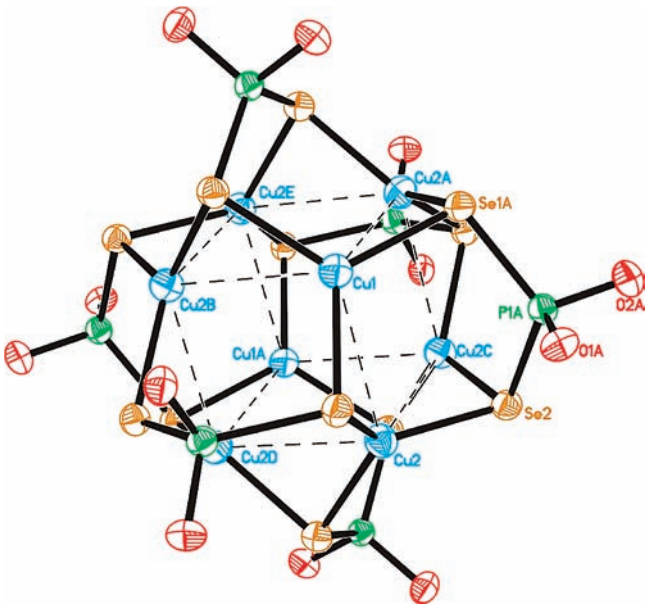

Figure 1. Structure of dication of **1**, $Cu_8[Se_2P(O^iPr)_2]_6^{2+}$ (30% thermal ellipsoid), with isopropyl groups omitted for clarity. Selected bond lengths (Å) and angles (deg): Cu(2)···Cu(2C), 3.216(1); Cu(1)···Cu(2), 3.220(1); Se(1)−Cu(1), 2.3510(5); Se(1)−Cu(2), 2.3600(9); Se(2)−Cu(2), 2.3560(8); Cu(1)−Se(1B), 2.3509(5); Cu(1)−Se(1A), 2.3511(5); Cu(2)−Se(2D), 2.3520(9); Se(1)−P(1), 2.1861(13); Se(2)−P(1A), 2.1941(14); Cu(1)−Se(1)−Cu(2), 86.25(4); Cu(2)−Se(2)−Cu(2C), 86.17(3); Se(1A)−P(1A)−Se(2), 119.39(6).

pattern. Each Cu atom is trigonally coordinated by three Se atoms from three independent dsep ligands. Twelve selenium atoms from six dsep ligands are located in the vertices of a slightly distorted icosahedron, and an idealized T_h point group symmetry is exhibited. Thus six P atoms and 12 Se atoms of the ligands are symmetry-related and reflected nicely from its ^{31}P and ^{77}Se NMR studies (vide infra). Whereas the ligand "bite" distances of 3.782(1) Å and Cu−Se distances in the range of 2.3509(5)−2.3600(9) Å in **1** are normal and comparable with those in the reported anion-centered copper cubes,[20] the Cu···Cu distances in the range of 3.216(1)−3.220(1) Å are the maximum in the series (Table 1). Notably, most of the empty, cubic copper frameworks surrounded by chalcogen donor ligands are anionic.[29] The Cu−Cu distances in $[Cu_8(S_2C_4O_2)_6]^{4-}$, $[Cu_8\{S_2CC(CO_2Et)_2\}_6]^{4-}$, and $[Cu_8(i\text{-}MNT)_6]^{4-}$ were in the ranges of 2.787(2)−2.906(2), 2.782(3)−2.870(3), and 2.759(6)−2.882(6) Å, respectively.[30] With the cationic, cubic copper cage, the compound **1** is the third example next to $[Cu_8(S_2CNPr_2)_6]^{2+}$ and $[Cu_8(S_2PPh_2)_6]^{2+}$ without an encapsulated atom.[31,32] Both compounds showed a Cu_8^I cubic core stabilized by six monoanionic, dithio ligands in a tetrametallic-tetracoordinative (μ_2, μ_2) fashion via their 12 sulfur atoms. Cu−Cu distances in $[Cu_8(S_2CNPr_2)_6]^{2+}$ and $[Cu_8(S_2PPh_2)_6]^{2+}$ lie in the ranges of 2.8038(6)−2.8087(6) and 3.1596(13)−3.2861(14) Å, the latter of which involving a dichalcogenophosphine ligand and Cu−Cu distances are comparable to those identified in compound **1**.

Compound 2a. Each of the dsep ligands in **2a** showed a bonding pattern similar to that of **1**, and the Cu_8 core is inscribed into a slightly distorted Se_{12} icosahedral unit from six dsep ligands. However, the structure clearly shows that a fluoride is entrapped into the central Cu_8 cubic core with long Cu−F distances ranging from 2.584(2) to 2.694(1) Å (Figure 2). Interestingly, the Cu···Cu distances in **2a** [2.9702(18)−3.086(2) Å], approximately 0.2 Å shorter than those in **1**, indicate that contraction of the Cu_8 cubic core induced by the fluoride ion has occurred. Thus strong anion−cation interactions between the central fluoride and eight peripheral copper atoms are demonstrated. However, the Cu−Se distances [2.3544(14)−2.3766(13) Å] are comparable to those in **1**.

Compound 2b. The ethyl derivative of dsep ligand formed **2b**, having a structure very similar to that of **2a**, crystallizes with a solvated benzene. The central fluoride surrounded by eight copper in cubic arrangement that inscribed into a Se_{12} icosahedron also exhibits long Cu−F distances in the range 2.503(3)−2.685(7) Å. Cu···Cu distances along the edge of the cube [2.9113(16)−3.130(2) Å] are in the range of that observed in **2a** and are shorter compared to those in **1**. Cu−Se distances [2.3343(10)−2.3919(14)] are in their normal range and comparable to those observed in **1**.

From the comparison of metric data of three cationic, halide-centered cubic copper clusters surrounded entirely by diisopropyl diselenophosphate ligands (Table 1), it is clear that the Cu···Cu distances of a bromide-centered cube, $[Cu_8(Br)\{Se_2P(O^iPr)_2\}_6]^+$, already approach the limit of the empty cubic core in **1a**. These analyses clearly indicate that it is practically impossible to retain the cubic copper framework if the size of encapsulated anion is too big. Thus it is not surprising that the iodide anion can not be accommodated at the center of the cube.[33]

Compound 3a. The monocationic octanuclear copper cluster crystallizes in the monoclinic *C*2/*c* space group, which contains a tetracapped tetrahedral metallic core having T_d symmetry (Figure 3a) and is surrounded by six dsep ligands along with an interstitial hydride anion and the counteranion PF_6^-. A total of 16 copper atoms, each in 50% occupancy, form two cubes with one inside the other (Scheme 1) like those observed in $[Cu_8(H)\{S_2P(O^iPr)_2\}_6]^+$;[34] however, only four copper atoms in each cube are fully occupied as required by the symmetry. This tetracapped tetrahedral metallic core has only one homometallic predecessor, $[Cu_8(H)\{S_2P(O^iPr)_2\}_6]^+$, which involves the dithiophosphate ligand, its lighter congener.[34] The edge of the Cu_4 tetrahedron comprises Cu5A, Cu6, Cu7, Cu8 (abbreviated as Cu_v) atoms, and the Cu_v-Cu_v distances lie in the ranges from 2.928(4)−3.086(5) Å. However the distances between the capping Cu atoms (Cu1, Cu2A, Cu3A and Cu4A; abbreviated as Cu_{cap}) and the vertex of the triangular face which is being capped, i.e., Cu_v-Cu_{cap} distances, are in the range 2.701(3)−2.791(4) Å, which are shorter than the sum of the van der Waals radii for copper (2.80 Å).[35] Six dsep ligands, each retaining a tetrametallic, tetraconnective bonding mode, are located on the top of Cu_4 butterflies where hinge positions are edges of the tetrahedron and wingtips are four capping Cu atoms (Figure 3b). The dihedral angles of the Cu_4 butterflies are ∼153°. Unlike its precursor **1** that displays an almost identical Cu−Se bond length ∼2.355 Å, two kinds of Se−Cu distances, namely, Cu_v-Se and $Cu_{cap}-Se$, each averaging 2.560(3) and 2.307(2)

(29) Liu, C. W.; Staples, R. J.; Fackler, J. P., Jr. *Coord. Chem. Rev.* **1998**, *174*, 147–177.
(30) Hollander, F. J.; Coucouvanis, D. *J. Am. Chem. Soc.* **1977**, *99*, 6268–6280.
(31) Cardell, D.; Hogarth, G.; Faulkner, S. *Inorg. Chim. Acta* **2006**, *359*, 1321–1324.
(32) Assavathorn, N.; Davies, R. P.; White, A. J. P. *Polyhedron* **2008**, *27*, 992–998.
(33) Liu, C. W.; Hung, C.-M.; Wang, J.-C.; Keng, T.-J. *J. Chem. Soc., Dalton Trans.* **2002**, 3482–3488.
(34) Liao, P.-K.; Sarkar, B.; Chang, H.-W.; Wang, J.-C.; Liu, C. W. *Inorg. Chem.* **2009**, *48*, 4089–4097.
(35) Huheey, J. E. *Inorganic Chemistry: Principle of Structure and Reactivity*; Walter de Gruyter: Berlin, 1988; p, 278.

Table 1. Comparison of Selected Metrical Data (Å) of Cubal Clusters

	Cu−Cu (av)	Cu−X (av)	Cu−Se (av)	Se···Se (av)	X (radii)[23]	ref
$[Cu_8\{Se_2P(O^iPr)_2\}_6]^{2+}$, **1**	3.216−3.220 (3.218)		2.351−2.360 (2.355)	3.782 (3.782)		*a*
$[Cu_8(F)\{Se_2P(O^iPr)_2\}_6]^+$, **2a**	2.970−3.086 (3.040)	2.584−2.694 (2.632)	2.354−2.377 (2.367)	3.775−3.787 (3.781)	0.57(3)	*a*
$[Cu_8(Cl)\{Se_2P(O^iPr)_2\}_6]^+$	3.087−3.187 (3.137)	2.691−2.743 (2.719)	2.364−2.408 (2.385)	3.803−3.823 (3.812)	1.02(4)	15
$[Cu_8(Br)\{Se_2P(O^iPr)_2\}_6]^+$	3.139−3.225 (3.179)	2.733−2.771 (2.754)	2.374−2.399 (2.390)	3.816−3.833 (3.823)	1.20(3)	16
$[Cu_8(S)\{Se_2P(O^iPr)_2\}_6]$, **4**	2.7953−2.8474 (2.821)	2.3902−2.4607 (2.437)	2.4519−2.4673(2.458)	3.763 (3.763)	1.05(3)	*a*
$[Cu_8(Se)\{Se_2P(O^iPr)_2\}_6]$	2.859−2.974 (2.923)	2.506−2.577 (2.536)	2.428−2.474 (2.447)	3.765−3.793 (3.783)	1.20(4)	17

[a] Result is from this article.

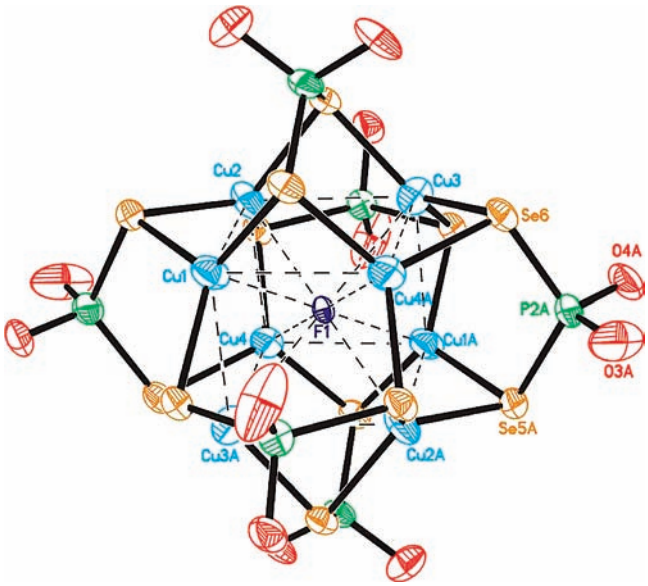

Figure 2. Structure of cationic $[Cu_8(F)\{Se_2P(O^iPr)_2\}_6]^+$ (30% thermal ellipsoid) in **2a** with isopropyl groups omitted for clarity. Selected bond lengths (Å) and angles (deg): Cu(3)−Cu(2), 3.086(2); Cu(1)−Cu(2), 3.0479(17); Cu(2)−Cu(4), 2.9702(18); Cu(1)−F(1), 2.694(1); Cu(2)−F(1), 2.584(2); Cu(3)−F(1), 2.650(2); Cu(4)−F(1), 2.600(1); Se(1)−Cu(3), 2.3702(14); Se(1)−Cu(2), 2.3766(13); Se(2)−Cu(4), 2.3544(14); Se(2)−Cu(2), 2.3756(14); Se(3)−Cu(1), 2.3692(14); Se(4)−Cu(1), 2.3671(14); Se(6)−Cu(3), 2.3678(13); Se(5)−Cu(1), 2.3683(13); Se(5)−Cu(2), 2.3763(14); Se−P, 2.168(3)−2.181(2); Cu−Se−Cu, 77.80(5)−81.09(5); Cu−Cu−Cu, 87.83(5)−92.14(5); Se−P−Se, 120.70(11)−121.08(10).

Å, are revealed in **3a** with the shorter one being associated to the wingtip Cu atoms (Cu_{cap}). Nevertheless, the average Se···Se "bite" distances of 3.749(6) Å in **3a** is only 0.033 Å shorter than those in its precursor. Unlike its precursor, **3a** contains only a single PF_6^- counteranion, which suggests that the charge of the cluster is +1. With the support of NMR data and the symmetry consideration (vide infra), a hydride was placed at the center of the cluster, i.e., at the center of Cu_4 tetrahedron, in order to balance the charge. The average Cu−μ_4-H distance [1.831(3) Å] is slightly longer than that observed in $H_6Cu_6[P(p\text{-tolyl})_3]_6$ [1.76(3) Å],[36] which was subjected to single-crystal neutron diffraction analysis to determine that six hydrides, each being 3-coordinate, are situated at face-bridging positions of the Cu_6 octahedron.

Compound 3b. The ethyl homologue that crystallizes in the trigonal $R\bar{3}c$ space group also displays a disorder of copper framework along the C_3 axis with the major component in 92% occupancy (Figure 4). The eight copper atoms are stabilized inside the Se_{12} icosahedron from six dsep ligands and form a tetracapped tetrahedron with an interstitial hydride that is not located in the crystallographic center of inversion. The vertex of the tetrahedron is formed by the Cu2, Cu2A, Cu2B, and Cu4 atoms, and the capping atoms are Cu1, Cu1A, Cu1B, and Cu3. The edge lengths of the tetrahedron (Cu_v−Cu_v), 2.860(2) and 3.015(2) Å, are larger than Cu_v−Cu_{cap} [2.6713(13)−2.7513(16) Å]; however, these distances are slightly less than those (Cu_v−Cu_v and Cu_v−Cu_{cap}) observed in **3a**, suggesting comparatively better packing in **3b**. Again like **3a**, all the dsep ligands show tetrametallic−tetraconnective (μ_2, μ_2) bonding mode to coordinate a Cu_4 butterfly formed by two Cu_{cap} and two Cu_v atoms. The average dihedral angle of the Cu_4 butterflies (∼153°) is almost identical to those in **3a**. The Cu_v−Se distances are slightly shorter and the Cu_{cap}−Se distances are longer in **3b** compared to those in **3a** (Table 2); however, the average Se···Se bite distance in the two compounds is comparable [**3a**, 3.749(6) Å; **3b**, 3.744(1) Å]. The average Cu−μ_4-H distance, 1.80(4) Å, is comparable to those observed in **3a**.

A C_3 rotational axis passing through the vertex of the tetrahedron, the central hydride, and a capping Cu atom opposite to the vertex and three C_2 axes, each being co-linear with two opposite P atoms and the central hydride, constitute an idealized T symmetry for the cluster cation in both **3a** and **3b**. Overall the T_h point group symmetry identified in **1** (also in **2a,b**) has been reduced to T symmetry in **3a** and **3b** as a result of the tetrahedral contraction of four of the eight copper atoms (vide infra) upon encapsulation of the hydride to create the dissymmetric molecules **3a,b**.

Recently we have reported structures of $[Cu_8(H)\{S_2P(OR)_2\}_6]^+$ (R = ^{i}Pr, Et), the hydride entrapped species in which the Cu_8^I core is inscribed inside a S_{12} icosahedron and each of the six dithiophosphate ligands donates two S atoms to exhibit an tetrametallic-tetracoordinate bonding pattern.[34] Both structures showed a tetracapped-tetrahedron Cu_8 core, similar to those observed in **3a,b**. The reference compounds also exhibited each of the dithiophosphate ligands coordinated to a Cu_4 butterfly with dihedral angle ∼155°. Cu_v−Cu_v distances in the isopropyl derivative and the major component of the ethyl homologue in the ranges of 2.908(2)−3.116(3) and 2.826(3)−3.128(4) Å, respectively, are comparable to those in the complexes involving their Se congener. The ranges of Cu_v−Cu_{cap} distances of the respective reference compounds, 2.6759(17)−2.7512(19) and 2.692(2)−2.842(3) Å, are also comparable to those in **3a** and **3b**. The average Cu−H distance in **3a**, 1.831(3) Å, is longer than that in its ethyl homologue **3b** [1.80(4) Å]; however,both of these distances are slightly shorter compared to Cu−H (av) in $[Cu_8(H)\{S_2P(O^iPr)_2\}_6]^+$ (1.84 Å) and $[Cu_8(H)\{S_2P(OEt)_2\}_6]^+$ (1.91 Å).

It is worthwhile to mention that a 4-coordinate hydrogen in the tetrahedral cavity of solid-state metal hydrides is not uncommon.[37] The first molecular compound containing a μ_4-H atom in tetrahedral geometry was reported in 1982 by Johnson

(36) Stevens, R. C.; McLean, M. R.; Bau, R.; Koetzle, T. F. *J. Am. Chem. Soc.* **1989**, *111*, 3472–3473.

(37) *Metal Hydrides*; Mueller, W. M., Blackledge, J. P., Libowitz, G. G., Eds.; Academic Press: New York, 1968.

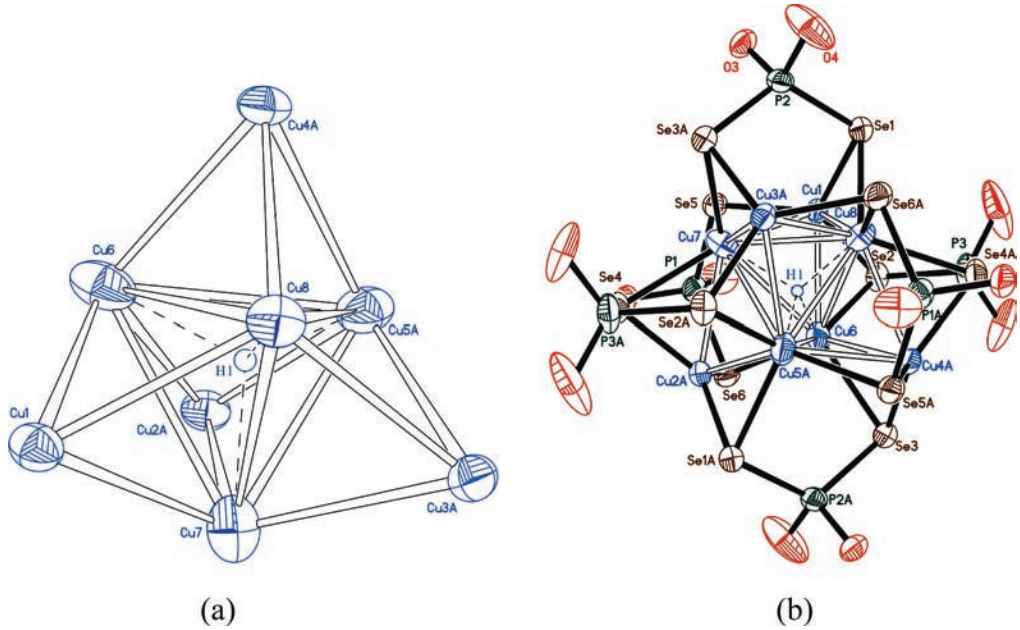

Figure 3. (a) Central unit $[Cu_8H]$ in **3a**. (b) Structure of the cationic $[Cu_4(\mu_4\text{-}H)(\mu_3\text{-}Cu)_4\{Se_2P(O^iPr)_2\}_6]^+$ (30% thermal ellipsoid) in **3a** with isopropyl groups omitted for clarity. Ranges of selected bond lengths (Å) and angles (deg): Cu−H, 1.762(3)−1.888(4); Cu_v−Cu_v, 2.928(4)−3.086(5); Cu_v−Cu_{cap}, 2.701(3)−2.791(4); Cu_v−Se, 2.543(3)−2.584(3); Cu_{cap}−Se, 2.278(2)−2.320(2); Se···Se (bite), 3.743(6)−3.754(3); Se−P, 2.162(2)−2.179(2); P−O, 1.548(7)−1.577(6); Se−P−Se, 119.00(11)−119.48(10); O−P−O, 105.7(5)−109.6(7). Cu_v = Cu atoms at the vertex of the tetrahedron; Cu_{cap} = Cu atoms capped to the tetrahedron face.

Scheme 1

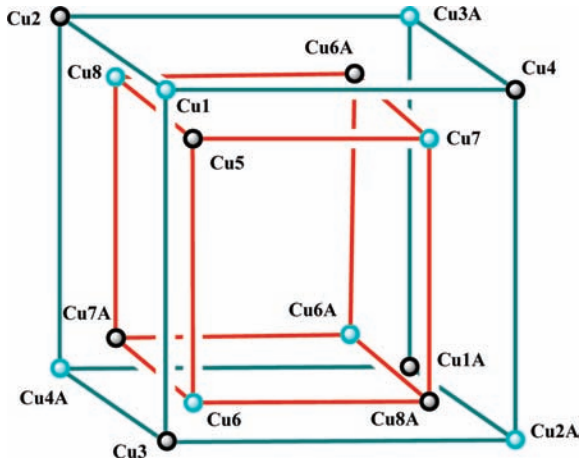

et al. in the complex $[HOs_{10}C(CO)_{24}]^-$.[38] Very recently it has been unambiguously located, by neutron diffraction, in the center of the tetrahedral metal complex $[Cp'YH_2]_4(THF)$ [Cp′ = $C_5Me_4(SiMe_3)$].[39] Also we have reported a 4-coordinate hydride encapsulated in $[Cu_8(\mu_4\text{-}H)\{S_2P(OR)_2\}_6]^+$, which is the sole example involving sulfur donor ligands.[34] Thus **3a,b** are the first to show a μ_4-H atom in the tetrahedral site of the copper cluster surrounded entirely by selenium donor ligands.

Homometallic clusters with a tetra-capped tetrahedral metal framework having an idealized T_d symmetry are virtually unknown, not to mention the anion-centered tetracapped tetrahedral, octametallic species. However, the symmetrical, heterometallic cluster, $Os_4(CO)_{12}[Pd(PBu^t_3)]_4$, an osmium tetrahedron capped by four palladium moieties, has been communicated by Adams and his co-workers.[40] A similar metal framework was identified in complexes of the type $[E_4\{Pd(PPh_2Me)_2\}_4]^{2+}$, E = Sb, Bi, where an idealized D_{2d} symmetry in the dicationic species was suggested.[41]

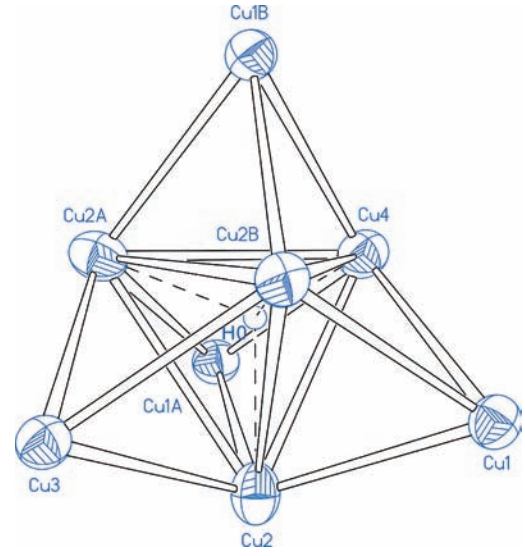

Figure 4. Central unit $[Cu_8H]$ in **3b**. Ranges of selected bond lengths (Å) and angles (deg): Cu−H, 1.63(12)−1.86(4); Cu_v−Cu_v, 2.860(2)−3.015(2); Cu_v−Cu_{cap}, 2.6713(13)−2.7513(16).

Compound 4. The sulfide-centered octanuclear copper cluster also shows a cubic geometry in the arrangement of metal centers (Figure 5). The compound **4** is iso-structural with the fluoride-

(38) Jackson, P. F.; Johnson, B. F. G.; Lewis, J.; McPartiln, M.; Nelson, J. H. *J. Chem. Soc., Chem. Commun.* **1982**, 49–51.
(39) Yousufuddin, M.; Gutmann, M. J.; Baldamus, J.; Tardif, O.; Hou, Z.; Mason, S. A.; Mclntyre, G. J.; Bau, R. *J. Am. Chem. Soc.* **2008**, *130*, 3888–3891.
(40) Adams, R. D.; Boswell, E. M.; Captain, B. *Organometallics* **2008**, *27*, 1169–1173.
(41) Stark, J. L.; Harms, B.; Guzman-Jimenez, I.; Whitmire, K. H.; Gautier, R.; Halet, J.-F.; Saillard, J.-Y. *J. Am. Chem. Soc.* **1999**, *121*, 4409–4418.

Table 2. Relevant Computed Results on the $[Cu_8(Se_2PH_2)_6]^{2+}$ and $[Cu_8(X)(Se_2PH_2)_6]^{+}$ (X = F, Cl, Br, H) Models Having T_h and/or T Symmetry

	$[Cu_8(Se_2PH_2)_6]^{2+}$	$[Cu_8(F)(Se_2PH_2)_6]^{+}$		$[Cu_8(Cl)(Se_2PH_2)_6]^{+}$	$[Cu_8(Br)(Se_2PH_2)_6]^{+}$	$[Cu_8(H)(Se_2PH_2)_6]^{+}$	
	T_h	T_h	T	T_h	T_h	T_h	T
relative energy, eV		0.04	0.00			0.54	0.00
HOMO−LUMO gap, eV		1.79	1.81	1.95	1.80	2.23	2.40
Cu−Cu (cube edge), Å	3.383	3.001	3.032[a]	3.217	3.280	2.601	2.709[a]
Cu−Cu (core tetrahedron edge), Å		4.244[b]	3.875			3.679[b]	2.869
Cu−X, Å		2.599	2.373	2.786	2.841	2.253	1.757
			2.837				2.730
Cu_1−Se, Å	2.383	2.411	2.438	2.414	2.421	2.464	2.574
			2393				2410
Se···Se, Å	3.922	3.870	3.871	3.928	3.951	3.825	3.817
relative energy of the $[Cu_8(Se_2PH_2)_6]^{2+}$ fragment, eV	0	0.28	0.47	0.15	0.16	1.00	0.95
bonding energy between the $[Cu_8(Se_2PH_2)_6]^{2+}$ and X^- fragments, eV		9.15	9.37	7.77	7.31	11.23	11.73
NBO population analysis of X		$2s^{1.97}\ 2p^{5.88}$	$2s^{1.98}\ 2p^{5.87}$	$3s^{1.95}\ 3p^{5.85}$	$4s^{1.95}\ 4p^{5.83}$	$1s^{1.63}$	$1s^{1.64}$

[a] Distorted cube. [b] Square face diagonal.

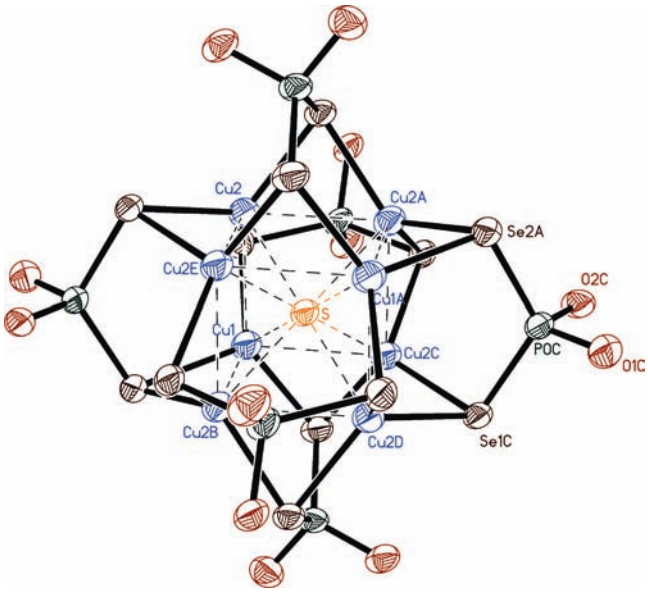

Figure 5. Structure of the $[Cu_8(\mu_8\text{-}S)\{Se_2P(O^iPr)_2\}_6]$ (30% thermal ellipsoid) in **4** with isopropyl groups omitted for clarity. Selected bond lengths (Å) and angles (deg): Cu(2)−Cu(2A), 2.8474(9); Cu(1)−Cu(2), 2.7953(9); Se(1)−Cu(2), 2.4519(8); Se(1)−Cu(2A), 2.4606(7); Se(2)−Cu(2), 2.4566(9); Se(2)−Cu(1), 2.4673(5); Cu(1)−S, 2.3902(12); Cu(2)−S, 2.4607(6); Se−P, 2.1648(14)−2.1761(12); Cu(2)−Se(1)−Cu(2A), 70.85(3); Cu(2)−Se(2)−Cu(1), 69.18(3); Se(1)−P−Se(2D), 120.18(6); Cu(2B)−Cu(1)−Cu(2), 91.78(3); Cu(1)−Cu(2)−Cu(2A), 89.286(19); Cu(2A)−Cu(2)−Cu(2D), 89.63(3).

centered clusters **2a,b** except that it is a neutral molecule. Cu···Cu distances along the edges are either 2.7953(9) or 2.8474(9) Å and are even shorter than the fluoride-centered **2a**, suggesting a greater amount of symmetrical, cubic contraction of the central Cu_8 framework induced by the dinegative sulfide anion. However, Cu−Se distances [2.4519(8)−2.4673(6) Å] are longer but Se···Se bite distances [3.763(1) Å] are slightly shorter than those in **1** and **2a**.

The insight revealed by the structural analysis that an icosahedral skeleton of 12 Se atoms inscribed a copper polyhedron (Figure 6) in both structures **1** and **3b** (or **3a**) strongly suggests that the tetrahedral contraction of four (depicted in red color) out of the eight copper atoms in the cube has taken place upon addition of a hydride. However, other anions such as fluoride or sulfide caused symmetrical, cubic contraction resulting in smaller Cu···Cu lengths as evident from Table 1. These observations lead us to propose two independent contraction pathways for the cubic copper framework upon anion encapsulation as shown in Scheme 2. Since the Cu···Cu bonding is weak in the series and the ligand bite effect does not allow very large shrinkage of the cube as observed in **2a**, the Cu−X (X = F, Cl, Br, H) bonding is likely to be the dominating factor. Overall a remarkable phenomenon that turns the O_h symmetry of a copper cube into the T_d symmetry of a tetracapped tetrahedron $[Cu_4(\mu_3\text{-}Cu)_4]$ core simply by the variation of the size of encapsulated anions is unique and to the best of our knowledge the first report in cluster chemistry. More importantly, the centrosymmetric character observed in cluster cations **1**, **2a,b**, and **4** (T_h) converts into the noncentrosymmetric structure in **3a,b** (T) without altering the conformation or bonding mode of the bridging ligand.

NMR Studies. Compound **1** displays a resonance frequency at 65.3 ppm flanked with a set of selenium satellites (626 Hz) in the ^{31}P NMR spectrum and a doublet peak centered at 89.9 ppm (J_{SeP} = 616 Hz) in the ^{77}Se NMR spectrum. Like the empty cluster **1**, all the anion-encapsulated compounds also exhibit a doublet in the ^{77}Se NMR spectrum and a singlet accompanied with selenium satellites in the ^{31}P NMR spectrum, originated from the dsep moieties. However, the observed resonance frequencies of anion encapsulated species (**2a**, **3a**, and **4**) shift downfield in the ^{31}P NMR spectrum and upfield in the ^{77}Se NMR spectrum in comparison with **1**. The ethyl homologue of these species (viz., **2b** and **3b**) show even more downfield shift in the ^{31}P NMR and more upfield shift in the ^{77}Se NMR spectrum (see Experimental Section). A singlet in the ^{31}P NMR and a doublet in the ^{77}Se NMR spectrum in all of the above complexes indicate that both P and Se atoms in all the clusters are chemically equivalent in solution.

Accordingly, the ^1H NMR spectrum displays a set of chemical shifts corresponding to the isopropyl or the ethyl groups for all of the compounds in the series. Furthermore a broad peak centered at −0.58 ppm that integrates to 1H relative to 12 methine protons of the isopropyl groups is observed in case of **3a** (Figure S1, Supporting Information). The broad peak did not change its shape but gradually shifted to −1.2 ppm upon slow cooling to 200 K. Thus this high field peak could be the resonance frequency of the hydride, and the peak broadening could be due to the coupling to quadruple nuclei of copper (I = 3/2). In a similar manner **3b** showed the encapsulated hydride resonance at −0.57 ppm. Furthermore, a broad peak at −0.54

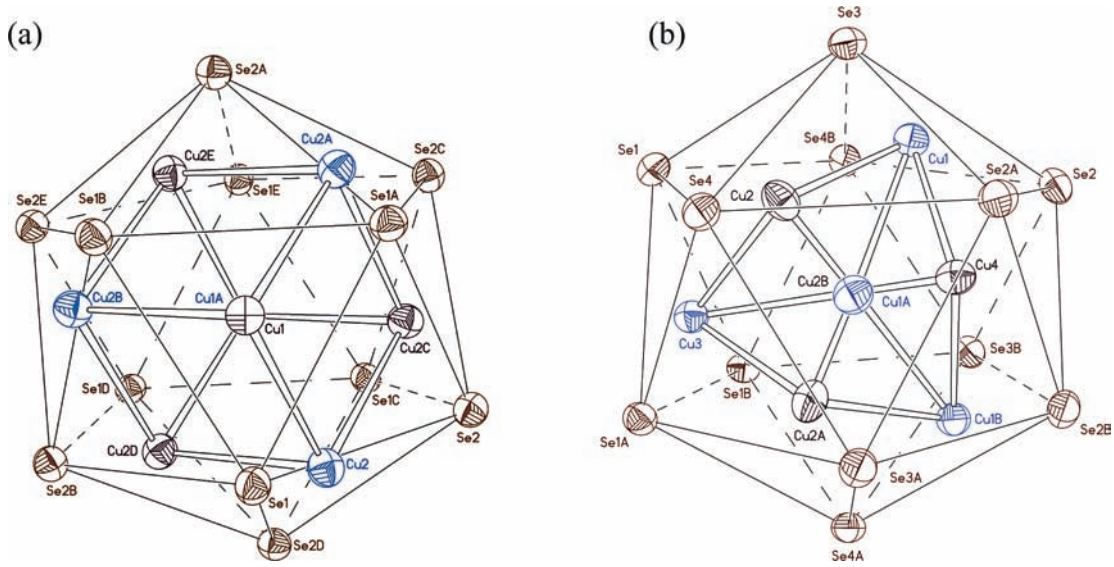

Figure 6. Schematic representations of the icosahedral arrangement of selenium atoms with an encapsulated copper polyhedron in structures **1** (a) and **3b** (b). The bonds between Se and copper atoms have been omitted for clarity.

Scheme 2

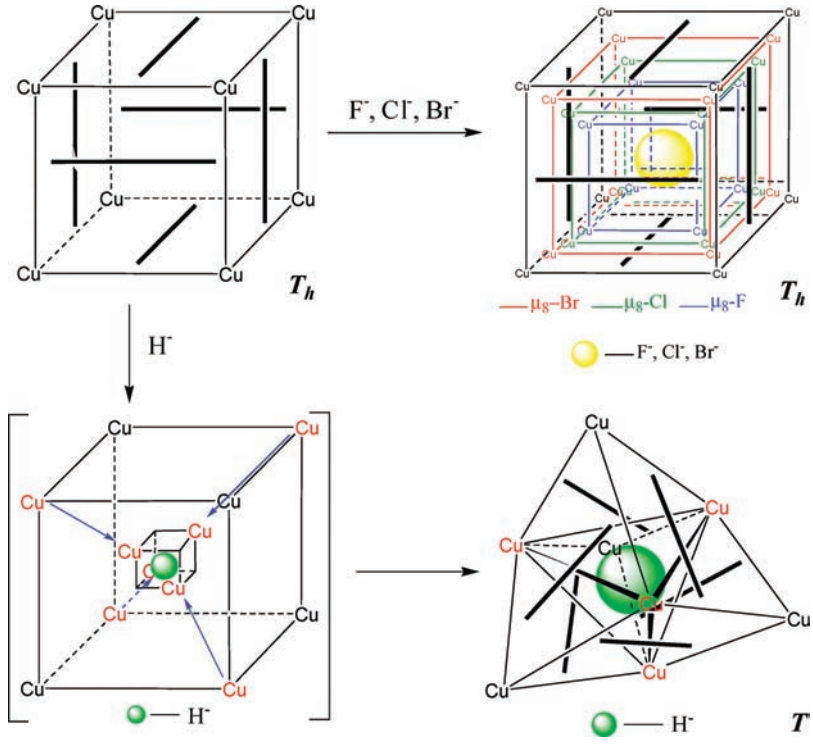

ppm revealed in ^{2}H NMR (Figure S2, Supporting Information) emphasizes the robust nature of this type of encapsulation reaction by confirming the formation of the deuteride-encapsulated species **3a′**. It might be worthy to note that both hydride and deuteride chemical shifts of the copper clusters involving dithiophosphate ligands were observed around 3.5−3.7 ppm. Since the size of the copper core around the hydride is almost identical in those dichalcophosphate ligands (vide supra), the chemical shift difference of the hydride (or deuteride) could be related to the different electron-donating ability between sulfur and selenium donors. This difference is nicely reproduced by DFT calculations on the model compounds $[Cu_8(H)\{Se_2PH_2\}_6]^+$ and $[Cu_8(H)\{S_2PH_2\}_6]^+$ for which the computed hydride chemical shift is 0.7 ppm for the former and 4.4 ppm for the latter (vide infra).

It has been reported that the chemical shift of interstitial hydrides in the solid state can vary over a range of +15.5 to −26.8 ppm, and it has been suggested that hydrides that are located in the center of a regular octahedron display the lowest-field chemical shifts, while those more asymmetrically oriented have high-field chemical shifts.[42] Thus this adds one more piece of evidence that the location of hydride at the center of two interpenetrated Cu_4 tetrahedra (Scheme 1) identified in compounds **3**, whose hydride resonance is not in the high field, is reliable.

Scheme 3

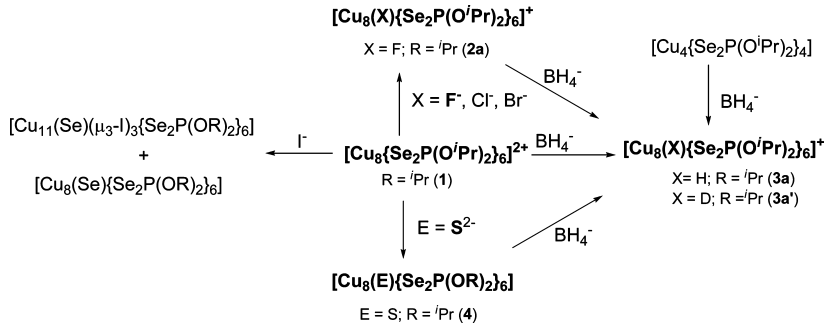

The resonance frequency of the central fluoride at −151.5 ppm in **2a** and −152.5 ppm in **2b**, respectively, is shifted ∼37 ppm upfielded relative to the Bu_4NF (δ, −115 ppm) in the ^{19}F NMR,[43] which confirms the presence of the encapsulated F^-. Surprisingly the ^{19}F chemical shift of the cluster $[Ag_{14}(C'C'Bu)_{12}F]^+$, which exhibits the entrapped fluoride within the Ag_8 cube, is at −65.7 ppm.[44]

Mass Spectrometry. The formation of all of the complexes was further verified by using mass spectrometry. Compound **1** exhibited the highest fragment peak corresponding to the adduct cation formulated as $[Cu_8\{Se_2P(O^iPr)_2\}_6(PF_6)]^+$ in the ESI-MS. On the other hand, MALDI-TOF mass spectrometry of the fluoride-encapsulated compounds, **2a** and **2b**, exhibited a molecular ion peak corresponding to the cationic cluster $[Cu_8(F)\{Se_2P(OR)_2\}_6]^+$ (R = ^{i}Pr and Et) to confirm their existence. In the case of **3a**, a band that can be formulated as $[Cu_8(H)\{Se_2P(O^iPr)_2\}_6]^+$ (m/z = 2350.50), is identified in the ESI-mass spectrum (Figure S3a, Supporting Information) with (−1) isotopic shift, which is consistent with the hydride encapsulated species. The molecular ion peak is magnified and presented in the inset of Figure S3a along with the theoretical isotopic distribution for comparison. Interestingly, **3a′** exhibits a peak for the $[Cu_8(D)\{Se_2P(O^iPr)_2\}_6]^+$ fragment that is exactly 1 mass unit (m/z = 2351.53) greater than that of **3a** in the positive ESI-mass spectrum (Figure S3b). Similar (−1) isotopic shifts in the mass spectrum for the hydride and deuteride encapsulated species were observed for their sulfur congeners $[Cu_8(H/D)\{S_2P(OR)_2\}_6]^+$.[34] In addition, **3b** exhibited the most intense peak corresponding to the cluster cation $[Cu_8(H)\{Se_2P(OEt)_2\}_6]^+$ in ESI-MS, and **4** showed the molecular ion peak for the entire cluster $[Cu_8(S)\{Se_2P(OEt)_2\}_6]$ in the MALDI-TOF mass spectrum.

Reactivity of the Clusters. The formation of the empty Cu_8 cluster (**1**) is highly facile. The reaction mixture was allowed to stir for 1 h for the completion of the reaction, but the reaction indeed proceeded far faster. Again the encapsulation reactions to form **3a** and **4** were also completed within few minutes, although the fluoride encapsulation in **1** to form **2a** took place in 1 day. On the other hand, it was also possible to obtain **2b** and **3b** by direct mixing of the copper source, dsep ligand, and the source of anion to be entrapped. Presumably the formation of empty copper cluster takes place first followed by the entrapment of the anion in situ. Thus, although we could not characterize the ethyl homologue of **1**, $(Cu_8L_6)(PF_6)_2$, beyond doubt because of unavailability of the crystallographic and mass spectrometric data, we intended to use the generality of these reactions to produce the anion encapsulated species involving the ethyl homologue of dsep ligand $[Se_2P(OEt)_2]^-$. Thus direct mixing of the dsep ligand, copper source, and the corresponding anion source could result in the formation of fluoride and hydride encapsulated species **2b** and **3b**. With the isopropyl derivative of dsep ligands, we demonstrated the formation of the fluoride-centered **2a**. In addition, previously reported $[Cu_8(X)\{Se_2P(O^iPr)_2\}_6]^+$ (X = Cl, Br) can also be prepared by adding proper anion source to **1** and could be confirmed by both the ^{31}P and ^{77}Se NMR spectra (Scheme 3). Interestingly, if **1** is dissolved in some chlorine-containing solvent such as $CHCl_3$ that may contain minute amount of HCl, a chloride-entrapped species was generated in a short time period. The reaction is so facile that it can be completed within 10 min, which was confirmed from the ^{31}P NMR by the addition of $CDCl_3$ to **1**. Another important fact is that the reaction of copper source and dsep ligand in 4:3 ratios produces **1**. The same reaction in a 1:1 ratio produced a tetra-nuclear cluster $[Cu_4\{Se_2P(^iPr)_2\}_4]$, while a 1:2 ratio produced selenide encapsulated species $[Cu_8(Se)\{Se_2P(O^iPr)_2\}_6]$. Thus when the ligand is in excess amount, the probable pathway of such a reaction is the formation of empty cluster followed by the abstraction of Se^{2-} from the partially decomposed dsep ligand. Again addition of the $NaBH_4$ (hydride source) to $[Cu_4\{Se_2P(^iPr)_2\}_4]$ leads to generation of a hydride entrapped **3a**. These facts mentioned above suggest the anion-entrapped species are more stable than the empty, octanuclear copper cluster. On the basis of the data in Table 1 we have proposed the contraction mechanism of the central Cu_8 core as emphasized in Scheme 2. Upon encapsulation of an anion, the repulsions between eight Cu^+ ions get minimized, which is evident from the near symmetrical shrinkage of the Cu_8 cube depending on the size and the charge of the central anion in the cases of Cl^-, Br^-, F^-, S^{2-}, and Se^{2-}. However, the smallest closed-shell anion, the hydride, does not induce a symmetrical cubic shrinkage of the metallic core; instead it undergoes a tetrahedral contraction (Scheme 2) which finally produced the tetracapped-tetrahedral core in **3a** and **3b**. It is noted that the dimension of bromide-centered cluster core approaches that of the empty cluster **1**, which may be the limit of an octanuclear copper core inscribed into a Se_{12} icosahedron without the presence of a central anion to stabilize the copper core. Thus the larger iodide could not be placed at the center of the Cu_8 core of **1** upon addition of 1 equiv of Bu_4NI to an acetone solution of $[Cu_8\{Se_2P(O^iPr)_2\}_6](PF_6)_2$; instead the reaction mixture resulted in the appearance of two new peaks in the ^{31}P NMR spectrum, 73.0 (J_{PSe} = 671.0 Hz) and 76.2 (J_{PSe} = 644.9, 673.0 Hz) ppm, which suggest the formation of $[Cu_8(\mu_8$-

(42) Eguchi, T.; Heaton, B. T. *J. Chem. Soc., Dalton Trans.* **1999**, 3523–3530.
(43) Buslaev, Y. A.; Petrosyants, S. P. *Polyhedron* **1984**, *3*, 265–270.
(44) Rais, D.; Mingos, D. M. P.; Vilar, R.; White, A. J. P.; Williams, D. J. *J. Organomet. Chem.* **2002**, *652*, 87–93.

Table 3. Relevant Computed Results on the $[Cu_8(S_2PH_2)_6]^{2+}$and $[Cu_8(X)(S_2PH_2)_6]^+$ (X = F, Cl, Br, H) Models Having T_h and/or T Symmetry

	$[Cu_8(S_2PH_2)_6]^{2+}$	$[Cu_8(F)(S_2PH_2)_6]^+$		$[Cu_8(Cl)(S_2PH_2)_6]^+$	$[Cu_8(Br)(S_2PH_2)_6]^+$	$[Cu_8(H)(S_2PH_2)_6]^+$	
	T_h	T_h	T	T_h	T_h	T_h	T
relative energy, eV		0.01	0.00			0.42	0.00
HOMO−LUMO gap, eV	2.43	2.28	2.43	2.39	2.24	2.73	2.86
Cu−Cu (cube edge), Å	3.208	2.976	2.985[a]	3.164	3.219	2.614	2.688[a]
Cu−Cu (core tetrahedron edge), Å		4.209	3.984	4.474	4.553	3.697[b]	2.899
Cu−X, Å		2.577	2.440 2.715	2.740	2.788	2.264	1.776 2.695
Cu−S, Å	2.266	2.287	2.301 2.277	2.298	2.307	2.334	2.444 2.290
S···S, Å	3.596	3.582	3.911	3.628	3.646	3.550	3.542
relative energy of the $[Cu_8(S_2PH_2)_6]^{2+}$ fragment, eV	0	0.16	0.26	0.12	0.18	1.11	1.05
bonding energy between the $[Cu_8(S_2PH_2)_6]^{2+}$ and X^- fragments/eV		9.32	9.42	7.77	7.20	11.34	11.71
NBO population analysis of X		$2s^{1.97}\ 2p^{5.88}$	$2s^{1.98}\ 2p^{5.88}$	$3s^{1.95}\ 3p^{5.86}$	$4s^{1.95}\ 4p^{5.84}$	$1s^{1.64}$	$1s^{1.63}$

[a] Distorted cube. [b] Square face diagonal.

Se){$Se_2P(O^iPr)_2$}$_6$][17] and $[Cu_{11}(\mu_9\text{-Se})(\mu_3\text{-I})_3\{Se_2P(O^iPr)_2\}_6]$,[33] respectively. The undecanuclear copper cluster, $[Cu_{11}(\mu_9\text{-Se})(\mu_3\text{-I})_3\{Se_2P(O^iPr)_2\}_6]$, was, however, reported to be prepared by direct mixing of $Cu(CH_3CN)_4PF_6$, dsep ligand, and Bu_4NI in a 2:3:2 ratio.[33]

However, the most important phenomenon in this context might be the facile, irreversible replacement of other encapsulated anions by the hydride (or deuteride) (Scheme 3). Thus cubic copper complexes having an interstitial chloride (or bromide, fluoride, sulfide, selenide) anion undergo tetrahedral contraction upon reaction with BH_4^- to produce the most stable configuration of an octanuclear copper complex in the series, which is the hydride-centered, tetracapped-tetrahedral Cu_8 cage inscribed into 12 Se atoms. Stability of the hydride-centered complexes, **3a,b**, in the presence of large excess of those anions (F^-, Cl^-, Br^-, S^{2-}) can be an approximate estimation of the thermodynamic stability of the clusters. Furthermore the failed H^-/D^- exchange in the compounds **3** could be due to the localization of hydride at the cluster core, which is completely sheared by both copper atoms and dsep ligand units and the higher thermodynamic stability of these compounds as well. The increase in stability of the complexes upon such contractions of the core is further supported by the theoretical studies.

Theoretical Analysis. Following previous theoretical studies on related compounds,[45,46] a DFT investigation has been undertaken on the simplified model series $[Cu_8(X)(E_2PH_2)_6]^+$ (X = F, Cl, Br, H; E = Se, S) and on the parent empty cluster $[Cu_8(E_2PH_2)_6]^{2+}$. Relevant results are given in Tables 2 (E = Se) and 3 (E = S). Geometry optimizations were carried out assuming both T_h and T geometry constraints. Whereas in the case of $[Cu_8(E_2PH_2)_6]^{2+}$ and $[Cu_8(X)(E_2PH_2)_6]^+$ (X = Cl, Br; E = Se, S), the optimized T structure was found to be identical to the T_h one, in agreement with the experimentally observed centrosymmetric or pseudocentrosymmetric nature of **1** and $[Cu_8(S_2PPh_2)_6]^{2+}$,[32] it converged to a different one when X = F or H. In the case of $[Cu_8(F)(Se_2PH_2)_6]^+$, the T structure was found to be a true minimum on the potential energy surface, whereas the T_h one was not (largest imaginary value = 79i cm^{-1}). Consistently, the T structure was found to be more stable than the T_h one, but by only 0.04 eV. This value is hardly significant at the considered levels of theory and modelization. Nevertheless, although almost iso-energetic, the T_h and T structures differ significantly in shape, as exemplified by the tetrahedral distortion exhibited by the T geometry. Although still much larger than the "cube" edge (3.032 Å), the short tetrahedron edge (3.875 Å) indicates a contraction of 9% with respect to the corresponding value in the regular cubic (T_h) optimized structure ($3.001 \times \sqrt{2} = 4.244$ Å). The consequence of this tetrahedral distortion of the Cu_8 cube splits the 8 Cu−F distances into a set of four short (2.373 Å) and a set of four long (2.837 Å) distances. A very similar situation occurs in the case of the dithiophosphate derivative $[Cu_8(F)(S_2PH_2)_6]^+$, in which the computed true minimum is of T symmetry, exhibiting a tetrahedral contraction of 5% and lying 0.01 eV below the T_h structure for which the largest computed imaginary frequency is equal to 71 i cm^{-1}. In that particular case, the two sets of Cu−F distances (2.440 and 2.715 Å) are less different than in the diselenophosphate case. Clearly, in the case of X = F and contrarily to the cases of X = Br and Cl, there is a flat potential energy surface over a large range of reaction coordinates along the T_h to T distortion both in the diselenophosphate and dithiophosphate series. This suggests that although the experimental structures of compounds **2a** and **2b** do not exhibit any significant tetrahedral distortion, it might be possible to isolate a $[Cu_8(F)\{E_2P(OR)_2\}_6]^+$ (E = Se, S) species that could exhibit a molecular architecture best described as a T rather than a T_h architecture. Nevertheless, considering the optimized T_h geometries, the experimentally observed cubic contraction within the Br, Cl, F series (Scheme 2) is nicely reproduced by the calculations, with a Cu−Cu cube edge distributed from 3.280 to 3.001 Å within the diselenophosphate series and from 3.219 to 2.976 Å within the dithiophosphate series. In case of E = Se, the computed cube edge is the largest for the empty $[Cu_8(E_2PH_2)_6]^{2+}$ cluster (3.383 Å), whereas for E = S the empty cluster is slightly more contracted than when bromine is incorporated (3.208 Å). It should be also mentioned at this point that all our attempts to optimize the iodide derivative $[Cu_8(I)(Se_2PH_2)_6]^+$ failed to converge, likely because the anionic radius of iodide is too large for the cubic cage to be able to house it. This is consistent with the fact that any attempt to synthesize a related iodide-centered Cu_8 compound has not succeeded so far.

The (very small) energetic preference computed for the T structure in the case of X = F is related to the fluorine size. In the case of the smaller X = H case, this preference is strongly reinforced and the associated tetrahedral contraction is much more pronounced. In the diselenophosphate model $[Cu_8(H)(Se_2PH_2)_6]^+$, the optimized T geometry is computed to be more

(45) Garland, M. T.; Halet, J.-F.; Saillard, J.-Y. *Inorg. Chem.* **2001**, *40*, 3342.
(46) Liu, C. W.; Hung, C.-M.; Santra, B. K.; Wang, J.-C.; Kao, H.-M.; Lin, Z. *Inorg. Chem.* **2003**, *42*, 8551–8556.

stable than the optimized T_h one by 0.54 eV, the latter not being a minimum on the potential energy hypersurface (largest imaginary frequency = 391 i cm^{-1}). The tetrahedral contraction is large (22%), inducing the existence of two very different sets of Cu−H distances (1.757 and 2.730 Å). Clearly, in this optimized model, the hydrogen atom is tetracoordinated. Calculations carried out on the dithiophosphate model $[Cu_8(H)(S_2PH_2)_6]^+$ lead to almost the same results (Table 3) with Cu−H distances of 1.776 and 2.695 Å. These results are in full agreement with the experimental structures of **3a**, **3b**, and $[Cu_8(H)\{S_2P(O^iPr)_2\}_6]^+$.[34]

For each member of the computed series $[Cu_8(X)(E_2PH_2)_6]^+$ (X = F, Cl, Br, H; E = Se, S), the energy of the empty cage $[Cu_8(E_2PH_2)_6]^{2+}$ has been calculated in its frozen fragment geometry, relative to that of its energy minimum resulting from a full geometry optimization (Tables 2 and 3). In most of the compounds, the $[Cu_8(E_2PH_2)_6]^{2+}$ relative energy is on the order of a few tenths of eV. This is indicative of a large geometrical flexibility for the $[Cu_8(E_2PH_2)_6]^{2+}$ cage, which is the consequence of the weak Cu(I)−Cu(I) (d^{10}−d^{10}) bonding.[45,46] In the halogen series, the largest values are found for the tetrahedrally distorted fluoride species. However, the energy required for distorting the $[Cu_8(E_2PH_2)_6]^{2+}$ cage is overtaken by its bonding energy with the fluoride anion. Only in the case of the hydride species, the relative energy of the empty cage is on the order of 1 eV, because of the large cage contraction that is required for the building of Cu−H bonds, both in the T_h and T symmetries. Nevertheless, despite this significant destabilization of the cage, its bonding energy with H^- largely prevails (vide infra).

The bonding energy between the $[Cu_8(E_2PH_2)_6]^{2+}$ and X^- fragments, calculated as the difference between the energy of $[Cu_8(X)(E_2PH_2)_6]^+$ and the sum of the energies of its $[Cu_8(E_2PH_2)_6]^{2+}$ and X^- fragments, is given in Tables 2 and 3. It is noteworthy that the E = Se and E = S series provide very similar values. The largest bonding energies are obtained for X = H and are larger for the T structure than for the T_h structure, consistent with the fact that the former is the energy minimum. In the case of the halogen series, the bonding energy decreases in the order $F^- > Cl^- > Br^-$. In the fluoride case, it is larger for the T minimum, as in the hydride species.

The nature of the bonding between the $[Cu_8(E_2PH_2)_6]^{2+}$ and X^- fragments is expected to exhibit both significant ionic and covalent characters, as it has been shown in related dithiolato Cu(I) cubic clusters.[45] The covalent interaction can be described by the simplified interaction diagram shown in Figure 7. The empty cube $[Cu_8(E_2PH_2)_6]^{2+}$ possesses a set of eight accepting orbitals that are combinations of the eight individual accepting orbitals on each of the tricoordinated 16-eletron Cu(I) centers. These orbitals are made of Cu(I) σ-type $3dz^2$, $4p_z$, and 4s contribution and point toward the cube center. Among their eight combinations, only four have the proper symmetry (a_g and t_u in T_h symmetry) to interact with the ns and np orbitals of an incorporated halide anion. When the incorporated anion is a hydride, only the a_g interaction is present. This general bonding picture remains merely unchanged in the tetrahedrally distorted structure of T symmetry, the major effect of the T_h to T distortion being to localize the four crucial copper accepting orbitals on the Cu_4 core tetrahedron. In any cases, the strength of the covalent interaction is directly related to the electron transfer from the valence orbitals of the saturated anion into the accepting orbitals of the $[Cu_8(E_2PH_2)_6]^{2+}$ cage.

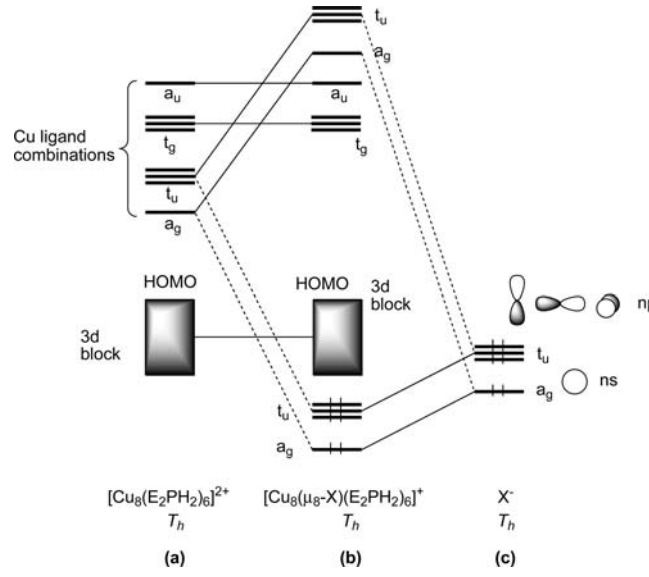

Figure 7. Simplified MO diagram describing the covalent interaction between the $[Cu_8(E_2PH_2)_6]^{2+}$ and X^- fragments in $[Cu_8(\mu_8\text{-}X)(E_2PH_2)_6]^+$ (X = halide; E = Se, S; T_h symmetry assumed). In the case of X = H, there is no t_u interaction.

The natural orbital population analysis (Tables 2 and 3) indicates a significant covalent interaction in the hydride case, with a transfer of 0.36 electron to the copper cage in both E = Se and E = S species. In the halide case, this transfer is always lower than 0.22, with a very small ns participation. Thus, the strength of the covalent interaction is weak in the halide cases as compared to the hydride species and decreases in the order Br > Cl > F. Therefore, the bonding of F^- with $[Cu_8(E_2PH_2)_6]^{2+}$ is essentially ionic in character, whereas that of H^- is significantly more covalent.

Concluding Remarks

High tendency to entrap anions from solvent molecule was the main obstacle to characterize the species of **1**. The cubic copper framework surrounded by 12 Se atoms does not undergo any sort of unsymmetrical distortion in the presence of entrapped halide or chalcogenide anion. Strong electrostatic (sometimes covalent) interactions between the central anion and peripheral copper atoms cause spherical distortion resulting in the cubic contraction (Scheme 2) of the octanuclear cubic copper core depending on the size and charge of the anions. In the case of encapsulation of the smallest closed-shell anion, hydride (or deuteride), the observed contraction is tetrahedral in nature. DFT calculations on a series of model compounds reproduce this tetrahedral contraction nicely in the case of hydride, which is related to the smaller size of the encapsulated anion. In case of fluoride, the tetrahedrally contracted structure was computed to lie at almost the same energy as the cubic one, suggesting both structural types (T or T_h) could exist depending on the nature of the bridging ligands, although only symmetric architectures have been characterized so far. Since it will adopt the tetrahedral contraction for the interstitial hydride located in the center of the cube, there is no doubt about the observed disordered copper framework in the solid state as depicted in Scheme 1.

The consideration of the charge balance is an important factor to determine that the central atom is the hydride in compounds **3** besides the hydride (or deuteride) resonance displayed in the ^1H (or ^2H) NMR spectrum (Figures S1, S2, Supporting Informa-

tion). What other anions with one negative charge could exist within ~1.8 Å away from Cu(I)? All Cu−F distances are longer than 2.5 Å in **2**, and the covalent radii of fluoride is even bigger than hydride.[26] The DFT calculation suggests that the Cu−H distance could be ~2.3 Å if the structure is cubic Cu_8H in T_h symmetry, which is 0.54 eV less stable than the tetracapped tetrahedral Cu_8H in T symmetry and which is not a local minimum on potential energy hypersurface.

The significance of this study is the change of shape from an empty or anion (halide or chalcogenide) encapsulated Cu_8 cube to a tetracapped tetrahedron core for encapsulated hydride (scheme 2). This sort of chemistry appears to be general for other dithio (or dithiolate) ligands.[34] The observation might have implications on the research of additives in the automobile industry, where Cu(I) and Zn(II) complexes of dithiophosphates are used as additives[47−50] to protect the engine presumably by encapsulating oxide and halides from the motor oil, but relatively little is known about the fundamental chemistry of such encapsulation.

Experimental Section

All chemicals were purchased from commercial sources and used as received. Solvents were purified following standard protocols.[51] All reactions were performed in oven-dried Schlenk glassware by using standard inert-atmosphere techniques. $NH_4Se_2P(O^iPr)_2$ and $NH_4Se_2P(OEt)_2$[52] were prepared according to the reported methods. All reactions were carried out under N_2 atmosphere by using standard Schlenk techniques. The elemental analyses were done using a Perkin-Elmer 2400 CHN analyzer. NMR spectra were recorded on Bruker Advance DPX300 FT-NMR spectrometer that operates at 300 MHz while recording ^{1}H, 121.5 MHz for ^{31}P, 57.2 MHz for ^{77}Se, 376.5 MHz for ^{19}F, and 46.1 MHz for ^{2}H. The ^{19}F{^{1}H}, ^{31}P{^{1}H}, and ^{77}Se{^{1}H} NMR are referenced externally against $CFCl_3$ (δ = 203.1 ppm), 85% H_3PO_4 (δ = 0 ppm), and PhSeSePh (δ = 463 ppm), respectively. The chemical shift (δ) and coupling constant (J) are reported in ppm and Hz, respectively. The NMR spectra were recorded at ambient temperature if not mentioned. Melting points were measured by using a Fargo MP-2D melting point apparatus. MALDI-TOF spectra were acquired using an Autoflex time-of-flight mass spectrometer (Bruker Daltonic, Bremen, Germany) equipped with a 337-nm nitrogen laser (10 Hz, 3-ns pulse width). ESI-mass spectra were recorded on a Fison Quattro Bio-Q (Fisons Instruments, VG Biotech, UK).

Safety Note. *Selenium and its derivatives are toxic! These materials should be handled with great caution.*

Synthesis. $[Cu_8\{Se_2P(O^iPr)_2\}_6](PF_6)_2$, 1. To a solution of $Cu(CH_3CN)_4PF_6$ (0.153 g, 0.41 mmol) in 30 mL of acetone was added $[NH_4Se_2P(O^iPr)_2]$ (0.100 g, 0.308 mmol) was added, and the mixture was stirred at room temperature for 1 h. It was then filtered to get rid of any solid, and the filtrate was evaporated to dryness under vacuum to get a blue solid, which was washed with deionized water and dried under vacuum to obtain $[Cu_8\{Se_2P(O^iPr)_2\}_6](PF_6)_2$ as yellowish-green powder. Yield: 0.108 g (82%). Mp: 84 °C. Anal. Calcd for $Cu_8H_{84}C_{36}O_{12}P_8F_{12}Se_{12}$: C, 16.37; H, 3.21. Found: C, 16.32; H, 3.43. ^{1}H NMR (acetone-d_6): 1.49 (d, $^3J_{HH}$ = 6.12 Hz, 72H, CH_3), 5.05 (m, 12H, CH). ^{31}P NMR (acetone-d_6): 65.3 (s, $^1J_{PSe}$ = 623.2 Hz, P($O^iPr)_2$), −143.0 (septet, $^1J_{PF}$ = 706.2 Hz, PF_6). ^{77}Se NMR (acetone-d_6): 90.0 (d, $^1J_{SeP}$ = 616.7 Hz). ESI-MS (m/z) (calcd): 2495.9 (2495.74) $[Cu_8\{Se_2P(O^iPr)_2\}_6](PF_6)^+$.

$[Cu_8(\mu_8\text{-}F)\{Se_2P(O^iPr)_2\}_6](PF_6)$, 2a. To a solution of $[Cu_8\{Se_2P(O^iPr)_2\}_6](PF_6)_2$ (0.301 g, 0.114 mmol) in 30 mL of acetone was added $Bu_4NF\cdot xH_2O$ (0.030 g, 0.114 mmol). The mixture was stirred at room temperature for 38 h. It was then filtered to get rid of any solid, and the filtrate was evaporated to dryness under vacuum to get a yellow powder. The powder was washed with deionized water and dried under vacuum to obtain $[Cu_8(F)\{Se_2P(O^iPr)_2\}_6](PF_6)$ as a brown solid. Yield: 0.227 g (79%). Mp: 83 °C (dec). Anal. Calcd for $Cu_8H_{84}C_{36}O_{12}P_7F_7Se_{12}\cdot H_2O$: C, 17.07; H, 3.42. Found: C, 16.72; H, 3.29. ^{1}H NMR (acetone-d_6): 1.49 (d, $^3J_{HH}$ = 6.27 Hz, 72H, CH_3), 5.04 (m, 12H, CH). ^{31}P NMR (acetone-d_6): 71.9 (s, $^1J_{PSe}$ = 642.6 Hz, P($O^iPr)_2$), −143.0 (septet, $^1J_{PF}$ = 707.8 Hz, PF_6). ^{77}Se NMR (acetone-d_6): 60.5 (d, $^1J_{SeP}$ = 640.6 Hz). ^{19}F NMR (acetone-d_6): −72.9 (d, $^1J_{FP}$ = 708.4 Hz, PF_6), −151.5 (Cu-μ_8-F). MALDI-TOF MS (m/z) (calcd): 2369.3 (2369.77) $[Cu_8(F)\{Se_2P(O^iPr)_2\}_6]^+$.

$[Cu_8(\mu_8\text{-}F)\{Se_2P(OEt)_2\}_6](PF_6)$, 2b. $Cu(MeCN)_4PF_6$ (0.336 g, 0.90 mmol), $NH_4[Se_2P(OEt)_2]$ (0.200 g, 0.67 mmol) was charged in a 100 mL Schlenk flask, and 30 mL of acetone was added to it. $Bu_4NF\cdot xH_2O$ (0.030 g, 0.112 mmol) was dissolved in 5 mL of deionized water and then transferred to the solution. The solution was stirred at room temperature for 1 h. The reaction mixture was filtered, and the filtrate was evaporated to dryness under vacuum to obtain brown solid. The solid was washed with deionized water and dried under vacuum to obtain $[Cu_8(F)\{Se_2P(OEt)_2\}_6](PF_6)$ as a brown powder. Yield: 0.205 g (78%). Mp: 133 °C (dec). Anal. Calcd for $Cu_8H_{60}C_{24}O_{12}P_7F_7Se_{12}\cdot 0.5(CH_3)_2CO$: C 12.89; H 2.67. Found: C 13.02; H 2.89. ^{1}H NMR (acetone-d_6): 1.34 (t, $^3J_{HH}$ = 7.02 Hz, 36H, CH_3), 4.11 (m, 24H, OCH_2). ^{31}P NMR (acetone-d_6): 78.3 (s, $^1J_{PSe}$ = 647.2 Hz, P($OEt)_2$), −143.0 (septet, $^1J_{PF}$ = 710.6 Hz, PF_6). ^{77}Se NMR (acetone-d_6): 33.6 (d, $^1J_{SeP}$ = 636.0 Hz). ^{19}F NMR (acetone-d_6): −72.4 (d, $^1J_{FP}$ = 711.6 Hz, PF_6), −152.5 (Cu-μ_8-F). MALDI-TOF MS (m/z) (calcd): 2199.1 (2201.45) $[Cu_8(F)\{Se_2P(OEt)_2\}_6]^+$.

$[Cu_4(\mu_4\text{-}H)(\mu_3\text{-}Cu)_4\{Se_2P(O^iPr)_2\}_6](PF_6)$, 3a. To a solution of $[Cu_8\{Se_2P(O^iPr)_2\}_6](PF_6)_2$ (0.300 g, 0.114 mmol) in 30 mL of THF was added $NaBH_4$ (0.005 g, 0.118 mmol) was added, and the mixture was stirred at room temperature for 15 min. The reaction mixture was filtered, and the filtrate was evaporated to dryness under vacuum to obtain brown solid that was washed with deionized water and dried under vacuum to obtain $[Cu_4(\mu_4\text{-}H)(\mu_3\text{-}Cu)_4\{Se_2P(O^iPr)_2\}_6](PF_6)$ as a brown powder. Yield: 0.248 g (87%). Mp: 89 °C (dec). Anal. Calcd for $Cu_8H_{85}C_{36}O_{12}P_7F_6Se_{12}$: C, 17.32; H, 3.43. Found: C, 17.38; H, 3.16. ^{1}H NMR (acetone-d_6): −0.58 (bs, 1H, μ_4-H), 1.45 (d, $^3J_{HH}$ = 6.33 Hz, 72H, CH_3), 4.84 (m, 12H, CH). ^{31}P NMR (acetone-d_6): 84.0 (s, $^1J_{PSe}$ = 634.7 Hz, P($O^iPr)_2$), −143.0 (septet, $^1J_{PF}$ = 708.0 Hz, PF_6). ^{77}Se NMR (acetone-d_6): 1.1 (d, $^1J_{SeP}$ = 636.0 Hz). ESI-MS (m/z) (calcd): 2350.5(2351.78) $[Cu_8(H)\{Se_2P(O^iPr)_2\}_6]^+$.

$[Cu_4(\mu_4\text{-}D)(\mu_3\text{-}Cu)_4\{Se_2P(O^iPr)_2\}_6](PF_6)$, 3a′. It was prepared in a similar fashion as **3a** by using $NaBD_4$ instead of $NaBH_4$. Yield: 0.238 g (84%). Mp: 86.9 °C (dec). Anal. Calcd for $Cu_8H_{84}DC_{36}O_{12}P_7F_6Se_{12}\cdot 5H_2O$: C, 16.71; H, 3.74. Found: C, 16.36; H, 3.67. ^{1}H NMR (acetone-d_6): 1.45 (d, $^3J_{HH}$ = 6.15 Hz, 72H, CH_3), 4.84 (m, 12H, CH). ^{2}H NMR (acetone-d_6): −0.54 (bs, 1 D). ^{31}P NMR (acetone-d_6): 83.8 (s, $^1J_{PSe}$ = 632.7 Hz, P($O^iPr)_2$), −143.0 (septet, $^1J_{PF}$ = 708.2 Hz, PF_6). ^{77}Se NMR (acetone-d_6): 1.5 (d, $^1J_{SeP}$ = 633.9 Hz). ESI-MS (m/z) (calcd): 2351.5 (2352.79) $[Cu_8(D)\{Se_2P(O^iPr)_2\}_6]^+$.

$[Cu_4(\mu_4\text{-}H)(\mu_3\text{-}Cu)_4\{Se_2P(OEt)_2\}_6](PF_6)$, 3b. $Cu(MeCN)_4PF_6$ (0.336 g, 0.90 mmol) and $NH_4[Se_2P(OEt)_2]$ (0.200 g, 0.67 mmol) wee dissolved in 30 mL of THF. $NaBH_4$ (0.005 g, 0.118 mmol) was added, and the mixture was stirred at room temperature for 15 min. The reaction mixture was filtered, and the filtrate was evaporated to dryness under vacuum to obtain brown solid that was washed with deionized water and dried under vacuum to obtain $[Cu_4(\mu_4\text{-}H)(\mu_3\text{-}Cu)_4\{Se_2P(OEt)_2\}_6](PF_6)$ as a brown powder. Yield: 85%. Mp: 89 °C (dec). Anal. Calcd for $Cu_8H_{61}C_{24}O_{12}P_7F_6Se_{12}\cdot$THF: C, 14.01; H, 2.90. Found: C, 14.18; H, 3.14. ^{1}H NMR (acetone-d_6): −0.57 (bs, 1H, μ_4-H), 1.41 (t, $^3J_{HH}$ = 6.96 Hz, 72H, CH_3),

(47) Colclough, T.; Gibson, F. A.; Marsh, J. F. U.S. Patent 4867890, 1989.
(48) Di Biase, S. A.; Davis, K. E. U.S. Patent 5171461, 1992.
(49) Salomon, M. F.; Davis, K. E.; Karn, J. L. Cahoon, John M. U.S. Patent 5486300, 1996.
(50) Ogano, S.; Kuribayashi, T. U.S. Patent 6207625, 2001.
(51) Perrin, D. D.; Armarego, W. L. F.; Perrin, D. R. *Purification of Laboratory Chemicals*, 2nd ed.; Pergamon Press: Oxford, 1980.
(52) Liu, C. W.; Shang, I.-J.; Hung, C.-M.; Wang, J.-C.; Keng, T.-C. *J. Chem. Soc., Dalton Trans.* **2002**, 1974–1979.

4.25 (m, 24H, CH_2). ^{31}P NMR (acetone-d_6): 90.2 (s, $^1J_{PSe}$ = 638.7 Hz, P(OEt)$_2$), −143.0 (septet, $^1J_{PF}$ = 708.7 Hz, PF_6). ^{77}Se NMR (acetone-d_6): −24.1 (d, $^1J_{SeP}$ = 639.3 Hz). ESI-MS (*m*/*z*)(Cal.): 2184.4 (2183.46) $[Cu_8(H)\{Se_2P(OEt)_2\}_6]^+$.

$[Cu_8(S)\{Se_2P(O^iPr)_2\}_6]$, 4. To a solution of $[Cu_8\{Se_2P(O^iPr)_2\}_6](PF_6)_2$ (0.300 g, 0.114 mmol) in 30 mL of acetone was added NaSH·xH$_2$O (0.007 g, 0.125 mmol) in 5 mL of deionized water, and the mixture was stirred at room temperature for 30 min. The reaction mixture was filtered, and the filtrate was evaporated to dryness under vacuum to obtain yellow solid. The solid was washed with deionized water and dried under vacuum to obtain $[Cu_8(\mu_8\text{-}S)\{Se_2P(O^iPr)_2\}_6]$ as a yellow powder. Yield: 0.121 g (68%). Mp: 115 °C (dec). Anal. Calcd for $Cu_8H_{84}C_{36}O_{12}P_6SSe_{12}\cdot(CH_3)_2CO$: C, 19.19; H, 3.72. Found: C, 18.94; H, 4.07. ^{1}H NMR (acetone-d_6): 1.37 (d, $^3J_{HH}$ = 6.18 Hz, 12H, *CH*$_3$), 4.48 (m, 2H, *CH*). ^{31}P NMR (acetone-d_6): 74.2 (s, J_{PSe} = 669.1 Hz, P(O^{i}Pr)$_2$). ^{77}Se NMR (acetone-d_6): −53.8 (d, J_{SeP} = 666.3 Hz). MALDI-TOF MS (*m*/*z*) (calcd): 2382.3 (2382.84) $[Cu_8(S)\{Se_2P(O^iPr)_2\}_6]^+$.

X-ray Crystallography. Single crystals suitable for X-ray diffraction were grown by diffusing hexane into an acetone solution of the compounds. Crystals were mounted on the tips of glass fibers with epoxy resin. Data were collected on a Bruker APEXII CCD diffractometer using graphite monochromated Mo Kα radiation (λ = 0.71073 Å). Absorption corrections for the area detector were performed with the program SADABS.[53] Structures were solved by direct methods and were refined against the least-squares methods on F^2 with the SHELXL-97 package,[54] incorporated in SHELXTL/PC V5.10.[55] Hydrogen atoms on the alkyl side chains were placed at idealized positions. The central H$^-$ of **3a** and **3b** (the hydride of **3b** is not located in the inversion center and its positions were refined) were fixed during the least-squares refinements. Selected crystallographic data are listed in Table S1 with metric data of **1**, **2a**, **2b**, and **4** in Table S2, and **3a** and **3b** in Table S3 in the Supporting Information.

Computational Details

DFT calculations were carried out using the Gaussian 03 package,[56] employing BP86 functionals,[57] and using the general triple-ξ polarized basis set, namely, the Def2-TZVP set from EMSL Basis Set Exchange Library.[58] All stationary points were fully characterized as true mimina via analytical frequency calculations. Geometries obtained from DFT calculations were used to perform natural orbital analysis by the NBO 5.0 program.[59] The gauge including atomic orbital (GIAO) method has been used to compute the ^{1}H chemical shifts, $\delta = \sigma^{TMS} - \sigma^{cluster}$, where σ^{TMS} and $\sigma^{cluster}$ are, respectively, the isotropic chemical shielding of ^{1}H in tetramethylsilane and in the $[Cu_8(H)(E_2PH_2)_6]^+$ (E = Se, S) cluster.

Acknowledgment. We thank Dr. Mitch Chiang in Academia Sinica for acquisition of ESI-mass spectra. Financial support from the National Science Council of Taiwan (NSC 97-2113-M-259-007 and 98-2911-I-259-002) and the Institut Universitaire de France (IUF) are gratefully acknowledged.

Supporting Information Available: X-ray crystallographic files in CIF format for compounds **1**, **2a**, **2b**, **3a**, **3b**, and **4**; Figures S1−S3; detailed ref 56; crystallographic data (Tables S1−S3); and Cartesian coordinates of all the DFT computed models (Table S4). This material is available free of charge via the Internet at http://pubs.acs.org.

JA904089T

(53) Included in *SAINT V4.043: Software for the CCD Detector System*; Bruker Analytical: Madison, WI, 1995.
(54) Sheldrick, G. M. *SHELXL-97: Program for the Refinement of Crystal Structure*; University of Göttingen: Göttingen, Germany, 1997.
(55) *SHELXL 5.10 (PC version): Program Library for Structure Solution and Molecular Graphics*; Bruker Analytical: Maidson, WI, 1998.
(56) Frisch, M. J.; et al. *Gaussian 03, Revision B.04*; Gaussian, Inc.: Pittsburgh, PA, 2003. A full reference for Gaussian programs is provided in Supporting Information.
(57) Perdew, J. P. *Phys. Rev. B* **1986**, *33*, 8822–8824.
(58) Weigend, F.; Ahlrichs, R. *Phys. Chem. Chem. Phys.* **2005**, *7*, 3297.
(59) Glendening, E. D.; Badenhoop, J. K.; Reed, A. E.; Carpenter, J. E.; Bohmann, J. A., Morales, C. M.; Weinhold, F. Theoretical Chemistry Institute, University of Wisconsin, Madison, WI, 2001; http://www.chem.wisc.edu/~nbo5.